RHEOLOGICAL AND STRUCTURAL CHARACTERISATION OF WHEY PROTEIN ACID GELS CO-STRUCTURED WITH CHIA (*Salvia hispanica L.*) OR FLAX SEED (*Linum usitatissimum L.*) MUCILAGE

Christos Soukoulis[1,*], Sébastien Cambier[1], Tommaso Serchi[1], Maria Tsevdou[3], Claire Gaiani[2], Pau Ferrer[1], Petros S. Taoukis[3] and Lucien Hoffmann[1]

[1]Luxembourg Institute of Science and Technology, Environmental Research and Innovation, 5 avenue des Hauts-Fourneaux, L4362, Esch-sur-Alzette, LUXEMBOURG

[2]Université de Lorraine, LIBio, Laboratoire d'Ingénierie des Biomolécules, 2 av de la Forêt de Haye, BP 20163, F-54505, Vandoeuvre lès Nancy, FRANCE

[3]National Technical University of Athens, School of Chemical Engineering, Heroon Polytechniou 5, 15780, Zografou Campus, Athens, GREECE

*Author to whom correspondence should be sent
Dr Christos Soukoulis
christos.soukoulis@list.lu

ABSTRACT

The effects of different plant seed mucilage (PSM) extracts, namely chia seed (CSM) and flaxseed (FSM), on the kinetics of δ-glucono-lactone induced acidification and gelation phenomena of whey proteins (5% w/w WPI) were investigated. The rheological and microstructural properties of mixed whey protein-PSM (0.05 to 0.75% w/w) cold-set gels produced at 30 or 37 °C were studied by means of oscillatory rheology and confocal microscopy. On exceeding 0.125% of PSM, a significant reduction of the gelation time due to the formation of loosely entangled whey protein soluble aggregates was observed. The impact of PSM on the gelation rates was closely related to the PSM type and concentration. CSM addition induced a gradual reduction of maximal gelation rate over the entire concentration range tested. On the other hand, FSM conferred a steep impedance of the gelation when exceeded 0.375%, which was associated with the occurrence of segregative phase separation. Fitting the elastic modulus – gelation time data to a model adapted to the Flory-Stockmayer theory, it was demonstrated that the presence of PSM inhibits the whey protein crosslinking capacity under both tested acidification regimes, leading to the formation of shorter protein crosslinks and therefore, to lower gel stiffness. However, the formation rate of elastically active chain networks was found to be increasing for CSM and FSM contents up to 0.5 and 0.25% respectively, suggesting a synergistic acid gel structuring effect of PSM under these conditions.

Keywords: cold-set gelation; seed coat mucilage; biopolymers; viscoelasticity; protein gel microstructure

52 1. INTRODUCTION

53 Owing to their particular texturising, structuring, stabilising and nutritional aspects, milk
54 proteins and polysaccharides constitute hydrocolloids of paramount importance in food product
55 innovation. The addition of polysaccharides in dairy food matrices aims primarily to the
56 increase in the macroviscosity of the serum phase and the hampering of protein instability such
57 as sedimentation (Goh, Sarkar, & Singh, 2008). Polysaccharide – milk protein interactions are
58 governed by the ability of the former to adsorb onto proteins, their surface charge (anionic,
59 cationic or non-ionic) and concentration as well as by extrinsic factors such as pH, temperature,
60 ionic strength and presence of cationic species (Syrbe, Bauer, & Klostermeyer, 1998). Non-
61 adsorbing polysaccharide – milk protein interactions are mainly repulsive inducing exclusion
62 of the individual biopolymer phases known as depletion flocculation (e.g. galactomannans);
63 however, phase separation can be obviated when the non-adsorbing polysaccharide exceeds a
64 certain (critical) concentration (Corredig, Sharafbafi, & Kristo, 2011; Syrbe et al., 1998). On
65 the other hand, adsorbing polysaccharides may lead to milk protein aggregative phenomena
66 due to bridging flocculation (Everett & McLeod, 2005; Girard & Schaffer-Lequart, 2008; Pang,
67 Deeth, & Bansal, 2015).

68 Whey protein acid gel development is considered a two-stage physicochemical process. First,
69 heat treatment of whey proteins, under low ionic strength and protein concentration ($C<C_g$)
70 conditions and far from the isoelectric point ($pH \gg pI \approx 5\text{-}5.1$), induces the formation of soluble
71 protein aggregates via covalent (i.e. disulphide bonding) interactions of protein oligomers
72 (Alting, Hamer, de Kruif, & Visschers, 2000; Nicolai, Britten, & Schmitt, 2011). It has been
73 demonstrated that the hydrodynamic radii and the morphological aspects of the protein
74 aggregates are strongly dependent on pH, ionic strength and α-lactalbumin content (Nicolai et
75 al., 2011). In a second stage, controlled *in situ* acidification using e.g. slow hydrolysing δ-
76 glucono-lactone (GDL) or lactic acid starter cultures, leads to non-covalently driven

interactions between free thiol groups and disulphide bonds favouring supramolecular bridging of the protein aggregates which eventually results in the formation of a three-dimensional gel network (Alting et al., 2000; Eissa & Khan, 2005). Owing to their sustained disintegration throughout orogastrointestinal transit, acid protein gels have shown promising potential as substrates for oral delivery of bioactive compounds and viable probiotic cells, suppressors of intragastric emptying etc. (Abaee, Mohammadian, & Jafari, 2017; Burgain, Corgneau, Scher, & Gaiani, 2015; Morell & Fiszman, 2017).

Food market globalisation, food security as well as consumers' awareness on food wholesomeness and health benefits conferring potential, have increased the demand for minimally processed, safe, sustainable and clean label ingredients without compromising in terms of technological and sensory characteristics. Plant origin mucilage i.e. the gelatinous material found in plant cladodes (e.g. aloe vera, Indian fig opuntia) or plant seed coat of the *Brassicaceae*, *Linaceae, Plantaginaceae* and *Lamiaceae* species has recently gained much attention as alternative biopolymer in food applications (Soukoulis, Gaiani, & Hoffmann, 2018). In general, plant seed mucilage (PSM) constitute two major polysaccharidic fractions: a) a pectin-rich primarily composed of rhamnogalacturonan I, and b) a hemicelluloses-rich comprising mainly arabinoxylans (AX) (Western, 2012). Owing to their chemical structure diversification, PSMs exert remarkable techno-functionality including thickening and gelling properties, texturising and fat mimicking capacity, interfaces adsorbing and stabilising ability etc. (Behrouzian et al., 2014; Cui et al., 2006; Naji-Tabasi & Razavi, 2017; Soukoulis et al., 2018). In addition, promising health benefits have been ascribed to food products enriched with PSMs such as modulation of the satiety cascade, control of the postprandial blood sugar and lipid levels, regulation of the gastrointestinal system and gut microbiota (Tamargo et al., 2018; Kay et al., 2017; Luo et al., 2018; Menga et al., 2017). Chia seed (*Salvia hispanica L.*) and flaxseed (*Linum usitatissimum L.*) mucilage extracts are among the most investigated

polysaccharides in terms of the technological and functional profile. Chia seed and flaxseed mucilage have been applied as structuring, texturising, fat mimetic and emulsifying agents in bakery and cereal (Fernandes & Salas-Mellado, 2017; Menga et al., 2017; Salgado-Cruz, Ramírez-Miranda, Díaz-Ramírez, Alamilla-Beltran, & Calderón-Domínguez, 2017), dairy products (Campos, Dias Ruivo, da Silva Scapim, Madrona, & de Bergamasco, 2016), food powders and particulates (Bustamante, Oomah, Rubilar, & Shene, 2017; Liu, Shim, Shen, Wang, & Reaney, 2017; Timilsena, Wang, Adhikari, & Adhikari, 2016) and edible film packaging (Capitani et al., 2016).

Hitherto, only a few studies have been carried out for investigating the structuring and stabilising ability of chia seed and flaxseed mucilage in dairy gels. The addition of flaxseed gum (0.1 to 0.5% w/w) in cold set (Na^+ and Ca^{2+} induced) whey protein gels has been associated with significant reduction of their mechanical (strain and stress at gel rupture) properties and water holding capacity due to the occurrence of phase separation between the biopolymers (Kuhn, Cavallieri, & da Cunha, 2011). Recently, Basiri et al., (2018) have assessed the stabilising and structuring potential of flaxseed gum (in the absence or presence of carboxymethylcellulose, CMC) in acid dairy gels induced via lactic acid fermentation. Flaxseed gum addition (0.6% w/v) was associated with a significant improvement of the starter culture cell viability throughout production and storage whereas it acted synergistically with CMC (0.3% w/v) in terms of acid gel viscosity, gumminess, and springiness. In the present work, we aimed to the mechanistic understanding of interactions of chia seed (CSM) and flaxseed (FSM) mucilage gums with whey proteins in GDL induced acid gels. The impact of the mucilage gums on the kinetics of acidification and gelation phenomena as well as the microstructural, physical and viscoelastic characteristics of the formed acid gels were investigated.

2. MATERIALS AND METHODS

2.1 *Materials*

Black chia seed (Biothentic, Auchan Srl., France) and flaxseed (BIOG Srl, Luxembourg) were purchased from the local market. Whey protein isolate (Lacprodan DI-9224, 92% protein, <0.2% lactose and milkfat) was obtained from Arla Foods A/S (Viby, Denmark). Delta-glucono-lactone (GDL), Calcofluor White and Fast Green FCF fluorescent stains were purchased from Sigma-Aldrich (Leuven, Belgium).

2.2 *Extraction, isolation and proximate analysis of the crude mucilage gums*

Chia seed mucilage (CSM) was extracted according to Goh et al., (2016) with minor modifications. In brief, 60 g of chia seeds were soaked at 50 °C overnight in 2 L of deionised MilliQ water (18 MΩ, Millipore, USA) buffered at pH = 8 using 1 M NaOH. A small amount of sodium azide (6 mM) was added in the seed suspension to prevent microbial growth. To avoid excessive contamination of the mucilage, no mechanical treatment of the seeds to partially dissociate the seat coat adherent mucilage was applied. The seed suspension was transferred to 50 mL centrifuge tubes and centrifuged at 4800 *g* for 20 min at room temperature and the supernatant containing the non-adherent mucilage was collected into a glass beaker. The crude mucilage was centrifuged at 10000 *g* for 15 min at room temperature to remove any proteinaceous or non-soluble impurities, mixed (1:3) with absolute ethanol and kept under magnetic stirring for 1 h at room temperature to allow polysaccharides aggregation. The ethanolic suspension was centrifuged at 4800 *g* for 10 min and the collected polysaccharide pellets were flushed under a nitrogen stream at 40 °C for 1 h (TurboVap, Biotage, Uppsala, Sweden). The pellets were reconstituted (*ca.* 1.5% w/v) in distilled water, vacuum concentrated at 60 °C (Rotavapor R-100, Büchi, Flawil, Switzerland), frozen at −80 °C overnight and eventually freeze-dried at −82 °C for 96 h (Christ, Alpha 1-2LD Plus, Germany). The lyophilisates were coarsely ground using a pestle and mortar and then finely powdered in a ball

mill (MM400, Retsch, Germany). The mucilage powders were sealed in glass vials and stored in dark at room temperature until further use. The same procedure was followed to isolate flaxseed mucilage (FSM) with the exception of buffering the seed suspension at pH = 7.

The chia and flaxseed mucilage gums obtained following the aforementioned procedure were analysed for proximate composition. In brief, the residual water, ash, total lipid and protein contents of the PSMs were determined following the 925.10, 942.05, 922.06 and 981.10 AOAC standardised procedures. The PSMs total carbohydrate content was determined using the Albalasmeh, Berhe, & Ghezzehei (2013) method, whereas the hexuronic (D-glucuronic and D-galacturonic) acids content was measured by means of K-Uronic 04/16 enzymatic kit (Megazyme Ltd., Wicklow, Ireland). CSM had the following composition (w/w): 6.1±0.1% residual water, 1.9±0.1% total lipids, 83.8±0.4% total carbohydrates, 4.3±0.5% protein and 3.9±0.1% ash. FSM had the following composition (w/w): 3.9±0.3% residual water, 1.1±0.1% total lipids, 83.6±0.7% total carbohydrates, 9.8±0.5% protein, and 1.6±0.1% ash. The total hexuronic acids contents were found to be 14.7 ± 0.2 and 22.4 ± 0.4 % w/w for CSM and FSM respectively.

2.3 *Preparation of the acid gels*

Direct acidified whey protein gels were produced as described in Meletharayil et al. (2015) with minor modifications. Whey protein isolate (WPI) was reconstituted (10% w/w) in distilled water, buffered at pH=7 with NaOH 0.5 M, hydrated for 1 h at 50 °C, heat-treated at 80 °C for 15 min to allow complete protein denaturation and rapidly cooled at 37 or 30 °C using an ice water bath. A small amount of sodium azide (0.02% w/w) was added in protein solutions to inhibit bacterial growth. Acid protein gels were prepared by blending the protein aliquot with a chia or flaxseed mucilage solution (1.5% w/w buffered at pH = 7 and pre-conditioned either at 37 or 30 °C) at given ratios to achieve a final 5% w/w protein and 0.0625-0.75% w/w chia mucilage content, and then 1.2% w/w of GDL was added to commence the *in situ* acidification.

177 The amount of GDL was calculated in order to ensure the completion of the hydrolysis of GDL
178 approximately at $pH_{end} = 4.5$.

179 2.4 *Acidification kinetics*

180 The pH decline throughout GDL hydrolysis to gluconic acid was monitored at 30 s time
181 intervals using a pH-meter (WTW, 3420-2, Weilheim, Germany). As hydrolysis of GDL is
182 mass transfer driven due to the occurrence of sol-gel phase transition, the pH data were
183 sequentially fitted to a first-order kinetic model assuming a burst (k_1) and sustained (k_2) GDL
184 hydrolysis stage as follows:

185 $$pH = pH_{\infty} + a \cdot \exp(-k_1 t) + b \cdot \exp(-k_2 t) \quad (1)$$

186 where pH_{∞}, denotes the end-point pH value (i.e. 4.5), a, b are constants whereas k_1, k_2 refer to
187 the decay constants as influenced by the sol-gel transitions. In order to have an overview of the
188 entire acidification process, the half mean time (τ_c) was calculated as follows:

189 $$\tau_c = \frac{\ln 2}{k_1 + k_2} \quad (2)$$

190 2.5 *Dynamic rheological measurements*

191 2.5.1 *Gelation kinetics*

192 The impact of CSM or FSM concentration on the kinetics of whey protein cold gelation was
193 studied by means of oscillatory rheology at either 30 or 37 °C. *In situ* acidification was carried
194 out in an Anton-Paar rheometer according to the procedure described in section 2.3 using a
195 concentric cylinder geometry (C-23C/T200/SS) of 27.1 mm diameter. To prevent water
196 evaporation a small amount of silicon oil was applied on the sample surface. Monitoring of
197 storage (G′) and loss moduli (G″) was carried out within the LVE region with the strain and
198 oscillation frequency values set at 0.5% and 1 Hz, respectively.

199 2.5.2 *Frequency sweep measurements*

200 After completion of gelation, the acid gels (prepared at either 30 or 37 °C) were cooled to 25

°C at the rate of 0.83 °C ·min^{-1}, kept isothermally for 30 min and then submitted to 0.01 – 100 Hz frequency sweeps at the LVE region (strain 0.5%). The frequency (*f*) dependence of the elastic modulus (G′) was calculated from the obtained rheological spectra according to the Winter-Chambon equation:

$$G' = K' \cdot \omega^{n'} \quad (3)$$

where K' is constant whereas n′ (0<n′<1) is a coefficient innate to viscoelastic behaviour (from ideal viscoelastic (n′=1) to true gel (n′=0) state) and $\omega = 2\pi \cdot f$ is the angular frequency (rad/s).

2.6 *Zeta-potential measurements*

The surface charge of the binary protein-mucilage aqueous systems was measured at 25 °C using Zetasizer Nano (Malvern Instruments, Worcestershire, UK). Prior to analysis, the systems were diluted (1:10) with phosphate buffer (5 mM, pH = 7.0). The electrophoretic mobility of the systems was calculated according to Henry's equation:

$$U = \frac{2 \cdot \varepsilon \cdot \zeta \cdot f(\kappa\alpha)}{3\eta} \quad (4)$$

where: ζ is the zeta-potential (mV), η (Pa·s) and ε denote the viscosity and permittivity of the whey protein/PSM dispersions, whereas the f(κα) parameters was assigned to value 1.5 according to Smoluchowski approximation (Liu et al., 2017).

2.7 *Visualisation of the whey protein/PSM dispersions and acid gels microstructure*

The microstructure of the acid gels as influenced by the PSMs presence and concentration was assessed by means of Confocal Laser Scanning Microscopy (CLSM, LSM 880 with airy scan, Zeiss, Jena, Germany) equipped with 40× objective lens. Acid gels were prepared by transferring 200 μL of whey protein/PSM dispersion into a 1.5 mL Eppendorf tube, mixed with 10 μL of Fast Green (0.05% w/w, FCF, Sigma Aldrich, Leuven, Belgium) and 10 μL of Calcofluor White (0.1% w/w, Brightener 28, Sigma Aldrich, Leuven, Belgium), vortexed for 30 s, transferred to an eight well Nunc Lab-Tek II chamber slide system (Thermofisher, Asse,

225 Belgium) and incubated in the dark at 30 °C for 1 h. In the case of the acid gels, the whey
226 protein/PSMs stained dispersions were mixed with 20 mg of GDL, vortexed for 60 s,
227 transferred to chamber slide systems and incubated in the dark at 30 °C for 3 h to allow
228 sufficient gel formation. Fast Green FCF and Calcofluor White were excited at 633 nm and
229 405 nm respectively and the emitted fluorescence was detected at 635-735 nm and 407-471
230 nm, respectively. CLSM micrographs were acquired at ambient (20 ± 2 °C) temperature.

231 2.8 *Water holding capacity of the acid gels*

232 The water holding capacity of the mucilage co-structured WPI acid gels (prepared at 30 °C)
233 was gravimetrically determined at 25 °C. In brief, gel samples were centrifuged at 10000 *g* for
234 10 min and water holding capacity (WHC) was calculated according to the formula:

235 $$\text{WHC } (\%) = 100 \cdot \frac{m_g - m_s}{m_g} \quad (5)$$

236 where m_g and m_s denote the amount (g) of the acid gel and the serum exudate.

237 2.9 *Statistical analysis*

238 Non-linear curve fitting regression analysis of the acidification (pH-t) and gelation (G* or G′,
239 t) data using the Marquardt-Levenberg method was performed using SigmaPlot v.12 software
240 (Systat Software Inc, San Jose, CA, USA).

241 The acidification and gelation kinetic parameters data were verified for fitting to the normal
242 distribution by means of the Shapiro-Wilk test and Q-Q plot representation whilst the variance
243 equality among the variables was verified using the Levene's criterion test. The significance of
244 the experimental parameters (mucilage type and concentration, incubation temperature) on the
245 acidification and gelation parameters was determined by means of three-way Analysis of
246 Variance (ANOVA). Tukey's multiple range test was used to separate means of data when
247 significant differences ($p<0.05$) were found. All univariate statistics were performed using
248 STATISTICA v.8 software (StatSoft Inc, Tulsa, OK, USA).

249

250 3. RESULTS AND DISCUSSION

251 3.1 *Impact of mucilage on acidification kinetics*

252 *In situ* acidification of dairy systems using GDL is generally ascribed to 1st order kinetics with
253 a pseudo-equilibrium usually to be achieved after 24-48 h (Cavallieri & da Cunha, 2008).
254 Parameters such as the incubation temperature, the milk protein type and concentration, the
255 presence of polyelectrolytes as well as the GDL content are known as primarily influencing the
256 acidification kinetics (de Jong et al., 2009; Lucey & Singh, 1997; Martin et al., 2009). Based
257 on the non-linear regression analysis results, the use of a single stage exponential decay model
258 did not allow us to achieve a satisfactory fitting of the experimental data particularly for pH
259 values beyond $pI_{WPI} \approx 5.2$ indicating that the kinetics of GDL hydrolysis might have been
260 influenced by the sol-gel phase transitions occurring due to whey protein aggregation.
261 According to the ANOVA results, the increase in incubation temperature led to a faster
262 ($p<0.001$) hydrolysis of GDL to gluconic acid, resulting in shorter times (2.58 and 2.20 h at 30
263 and 37 °C respectively) required for reaching the acidification end-point i.e. 4.5. Interestingly,
264 the k_1 and k_2 acidification rates were significantly ($p<0.001$) influenced by the PSM type and
265 concentration only in the systems incubated at 37 °C. The presence of FSM resulted in higher
266 acidification rates ($p<0.05$) compared to CSM i.e. 4.24 vs 4.14 h^{-1} and 0.097 vs 0.087 h^{-1} for k_1
267 and k_2 respectively. However, for both systems, a minimum amount of PSM (e.g. 0.25% w/w)
268 was required in order to detect significant ($p<0.05$) differences in the k_1 and k_2 values. Although
269 the existing literature data regarding the impact of anionic polysaccharides on the kinetics of
270 *in situ* GDL acidified milk protein systems are rather limited, it is assumed that the observed
271 differences in the acidification kinetics are associated with the ability of the anionic mucilage
272 polysaccharides to hold H^+ and to increase the microviscosity at the liquid-liquid interface. In
273 the presence of anionic polysaccharides, whey proteins may undergo soluble complex
274 formation (at $pH>pI_{WPI}$) via the electrostatic interaction between negatively charged chain

segments of the polysaccharides and positive charge bearing patches in the whey protein molecules such as amino, imidazole and guanidine groups (Girard, Turgeon, & Gauthier, 2002). It has been shown that the increase in the WPI to polysaccharide ratio (>10:1) and total surface charge density of the anionic polysaccharides may substantially influence the complexation of the latter to whey proteins (Girard & Schaffer-Lequart, 2008). According to the ζ-potential data, the increase in the CSM and FSM to WPI ratio (from 1:100 to 3:20) resulted in a significant increase in the absolute charge density of the binary blends, although no significant differences between CSM and FSM were detected, regardless their differing total hexuronic acid contents (14.67±0.06 and 22.44±0.19 g/100g respectively). This may be attributed to higher buffering capacity of FSM stemming from its higher protein content compared to CSM. The ζ-potential data were positively correlated (Suppl. Fig. 1) with k_2 values and negatively with k_1 values (only for 37 °C). According to the branching exponential model kinetic parameters (Table 1), the τ_c values ranged from 0.142 to 0.181 h corresponding to pH values ranging from 5.87 to 6.03 and 6.01 to 6.31 h for systems incubated at 30 and 37 °C, respectively. Girard & Schaffer-Lequart (2008) and Girard et al. (2002) studying the complexation of anionic exopolysaccharides (EPS) and low methylated pectins to whey proteins observed an initiation of the electrostatic interaction at values pH≈6 with the amount of the non-interacting whey proteins to be decreasing on temperature increase and pH decline, which generally corroborates our findings. Finally, the t_{acid} values (i.e. the time required to achieve pH = 4.5) were well correlated with ζ-potential and flow consistency coefficient (log$K$) of the WPI/PSM binary systems as shown in Suppl. Fig. 2. Although it is believed that the log$K$ dependence of t_{acid} is primarily associated with the extent of the PSM – whey proteins interactions, it is hypothesised that the PSM induced increase in the macroviscosity might have affected indirectly the overall acidification kinetics by sterically hindering the diffusion of gluconic acid at the liquid-liquid interface.

3.2 *Impact of mucilage on gel development kinetics*

The development of complex modulus G* of the WPI/PSM binary systems as a function of incubation time and pH is illustrated in Fig. 1. In most of cases, gelation time denotes the crossover point of the viscoelastic moduli i.e. $\tan\delta = G'/G'' = 1$. In the present work, the micro-gelled character of CSM endowed a well-defined viscoelastic behaviour in the initial WPI-CSM systems ($G' \approx G''$) and therefore, the calculated complex module ($G^* = \sqrt{(G')^2 + (G'')^2}$) values were fitted to a four parametric modified Gompertz model which has been previously used to describe the viscosimetric response of milk protein systems throughout lactic acid fermentation (Soukoulis, Panagiotidis, Koureli, & Tzia, 2007), as follows:

$$\log G^* = (\log G^*_{\infty} - \log G^*_{0}) \cdot \exp\left\{-\exp\left[\frac{\mu^{G^*} e}{(\log G^*_{\infty} - \log G^*_{0})}\right]\cdot(\lambda^{G^*} - t) + 1\right\} \quad (6)$$

where G^*_{∞}, G^*_0 denote the final and initial (pseudo-equilibrium) values of complex modulus, respectively, e is the Euler number, μ_{G^*} denotes the maximal gelation rate ($\log Pa \cdot s^{-1}$), λ_{G^*} is the gelation lag phase duration (s) and t is the incubation time (s).

As shown in Fig. 1, the gelation curves pattern was remarkably affected by the type and concentration of PSM. The gelation lag phase duration λ_{G^*} was significantly ($p<0.001$) influenced by the incubation temperature and PSM amount (Fig. 2). As expected, the increase in the incubation temperature led to the shortening of gelation lag phase duration by *ca.* 40% independently to the PSM type, but being significantly tuned by the PSM content. In the latter case, a minimum PSM to WPI ratio of 1:40 was required to detect a significant reduction of λ_{G^*}, whereas no lag phase was detected when PSM reached to 0.75% w/w. In agreement to the λ_{G^*} findings, the increase in the incubation temperature accelerated ($p<0.001$) the gelation process by *ca.* 15%. Interestingly, the responsiveness of the maximal gelation rate pattern to the PSM type and content was fairly diversified. Thus, the gelation rate remained constant for up to 0.375% of FSM followed by a steep reduction when exceeded the aforementioned level.

On the other hand, CSM affected adversely the μ values for the entire concentration range tested in this work. Parameters such as the acidification rate, the incubation temperature the protein content, the ionic strength and the presence of polysaccharides are known as impacting gelation rate (Cavallieri & da Cunha, 2008; de Jong et al., 2009; Liu et al., 2018; Pang, Deeth, & Bansal, 2015; Pang, Deeth, Sharma, et al., 2015). The λ_{G^*} values denote the time where gelation is initiated and therefore, both incubation temperature and mucilage presence were influencing parameters. According to the complex modulus – pH profiles (data not shown) when CSM or FSM was added up to the level of 0.125%, the gelation process was faster initiated compared to the WPI systems, which could be ascribed to the increase in the WPI soluble aggregates size in the presence of polysaccharides. Kharlamova et al. (2018) demonstrated that although the whey protein aggregates do not possess a determinant role on the acid gels viscoelastic properties, the gelation event may proceed rather faster when larger aggregates are formed after the heat treatment step. When CSM or FSM concentration exceeded 0.125%, a sharp shift of the pH_{gel} towards lower values was observed for both incubation temperature regimes. Thus, it is postulated that the increase in PSM to WPI ratio inhibits sterically the complexation of whey proteins to the anionic polysaccharide backbone and favours their intermolecular repulsion due to the excess of negative charge bearing carboxylic groups (Ye, 2008). Indeed, CLSM analysis of the microstructural aspects of FSM-WPI blends (Fig. 3B) gave support to the previous hypothesis; in general, a good thermodynamic compatibility with WPI was achieved for an FSM content up to 0.125%, whilst spontaneous segregative phase separation was occurred when FSM exceeded 0.125% w/w in accordance to previous studies (Corredig et al., 2011; Khalloufi, Corredig, Goff, & Alexander, 2009). On the contrary, CSM based systems did not exhibit any evident biopolymer depleted (WPI or mucilage) microdomains (Fig. 3A); instead, the presence of a rather continuous WPI microstructure with intruding microgelled CSM-rich patches was detected in agreement to the

observations of Goh et al. (2016). It is therefore assumed that as the CSM concentration increases the associative interactions between the whey protein aggregates is sterically inhibited, a mechanism that has been previously reported in anionic polysaccharide stabilised milk protein gels such as pectins and carrageenans (Everett & McLeod, 2005; Pang et al., 2015).

The determination of the fractal dimension of the whey protein aggregates by means of rheological, microstructural, light scattering or gel permeability data offer significant information about the interplay between the macroscopic properties of the protein gel and colloidal aspects of the protein aggregates (Ould Eleya, Ko, & Gunasekaran, 2004). On the other hand, models based on percolation or branching (cascade) theory can provide a satisfactory estimation of the mechanical properties of protein gels, especially close to the percolation threshold (Kavanagh, Clark, & Ross-Murphy, 2000).

In order to gain insight to the ability of whey protein monomers to undergo non-covalent crosslinking via sulfhydryl (–S–H) and disulphide bonds (–S–S–) throughout acidification, the storage modulus G′ data were fitted to an empirical low dimensional model previously used for investigating *in situ* sol-gel transition kinetics of biopolymers (Adibnia & Hill, 2016; Calvet, Wong, & Giasson, 2004) as follows:

$$G'(t) = G'_{\infty}\frac{t^{\alpha}}{t^{\alpha} + \theta^{\alpha}} \quad (7)$$

where G'_{∞} (in Pa·s) denote the elastic modulus at the pseudo-equilibrium (t_{acid}), t is the gelation time, θ is the gelation half-time (s), and α is a constant relative to the asymptomatic slope, P ($\frac{\alpha\, G'_{\infty}}{4\theta}$), at the gelation half-time. According the cascade theory (an extension of Flory-Stockmayer concept of gelation), the elastic modulus at the pseudo-equilibrium can be described as follows:

372 $$G'_{\infty} = \left\{N \cdot \frac{f}{2} \cdot a \cdot (1 - v)^2 \cdot (1 - \beta)\right\} \cdot P \cdot k \cdot T \quad (8)$$

373 where $N_e = \left\{N \cdot \frac{f}{2} \cdot a \cdot (1 - v)^2 \cdot (1 - \beta)\right\}$ denotes the number of the elastically active network chains

374 per primary volume, f is the number of sites among each molecule's length, a is the fraction of

375 the sites that have reacted, whereas v and β are parameters derived from cascade theory for gel

376 network formation (Lopes da Silva, Rao & Fu 1998).

377 At gelation half-time point, $P = \frac{\alpha\, G'_{\infty}}{4\theta}$, and hence, Eq. 8 can be written as follows:

378 $$G'_{\infty} = \frac{4\theta \cdot k \cdot T \cdot \dot{n}_e}{\alpha} \quad (9)$$

379 where: k is the Boltzmann constant and T (in K) is the incubation temperature and $\dot{n}_e$ ($mol \cdot s^{-1}$)

380 denotes the rate of elastically active network chains formed per whey protein aggregate

381 monomers volume (Lopes da Silva, Rao, & Fu, 1998).

382 As illustrated in Fig. 4, the gelation half-time values did not exert a clear response pattern to

383 PSM concentration (<0.5% w/w) with the gelation half-time values to oscillate around

384 1217±106 and 777±115 s at 30 and 37 °C, respectively. Corroborating the λ_{G*} values, the

385 increase in incubation temperature shortened significantly ($p<0.001$) the θ values. Suchlike to

386 the observations of Adibnia & Hill (2016), it is assumed that α can be used as a measure of the

387 whey protein crosslinking capacity. As clearly depicted in Fig. 4, the presence of PSM led to a

388 significant ($p<0.001$) reduction of α values, most likely due to the reduction of the sites number

389 allowing whey protein interaction via –S–S– and S–H. Interestingly, neither the PSM type nor

390 the incubation temperature were influential on α values.

391 At gelation half-time, the $\dot{n}_e$ values were varied according to the PSM type and concentration

392 as well as incubation temperature (Fig. 4). In CSM based systems, an increase in the $\dot{n}_e$ values

393 was observed when the WPI to mucilage ratio did not exceed 40:3 and 10:1 at 37 and 30 °C,

394 respectively. In the case of FSM, the gel elasticity synergism boundary was shifted to

395 remarkably higher WPI to mucilage ratios i.e. 40:1 to 40:3, as a result of the occurring
396 segregative phase separation. It should be noted that for WPI to FSM ratios exceeding 40:1,
397 the elastically active network formation rate was almost negligible for both tested incubation
398 temperatures, exerting a minor recovery of $\dot{n}_e$ values at the highest FSM content. On the other
399 hand, CSM addition did not compromise the formation of the elastically effective network
400 chains regardless the reduction of whey protein monomers crosslinking capacity. It is therefore
401 presumed that the microgelled structure conformation of CSM favours the overall gel elasticity
402 via an active filler related mechanism. The latter appears to be supported not only by the elastic
403 modulus values but also by the CLSM micrographs of the acid gels illustrating a satisfactory
404 protein adsorbing ability of CSM (Fig. 5 and Suppl. Fig. 3).
405 3.3 *Impact of mucilage on the mechanical and structural aspects of the acid gels*
406 The whey protein acid gels were pre-conditioned at 25 °C for 2 h prior to frequency sweep
407 rheological testing (Figs. 6 and 7). The individual WPI acid gels exerted significantly ($p<0.05$)
408 higher stiffness and elasticity when produced at lower incubation temperatures corroborating
409 previous findings (Lucey, 2002). As illustrated in Fig. 6, CSM addition imparted sufficient
410 structuring as indicated by the *ca.* 4-fold increase in the gels stiffness. Nevertheless, the
411 addition of CSM did not modify substantially the domineering weak gel viscoelastic behaviour
412 ($\tan\delta>0.1$) observed in WPI individual acid gels. CLSM analysis of the CSM based acid gels
413 (Fig. 5A), revealed a sufficient adsorption of mucilage components onto whey proteins as
414 evidenced by the purple coloured electrostatically complexed protein-polysaccharide
415 aggregates. Due to the selectivity of Calcofluor stain to the cellulosic fraction, we were not
416 able to justify the topological presence of pectinaceous RG-I matter e.g. found in the interspace
417 of the protein network or being stranded to the gel network. However, it is presumed that RG-
418 I fraction of mucilage would be also preferably adsorbed to whey proteins at $pH<pI_{WPI}$ as
419 demonstrated in previous studies regarding low methylated pectins (Everett & McLeod, 2005;

Wijaya, Van der Meeren, & Patel, 2017). On exceeding 0.25% w/w, blue stained micro-domains rich in hemicellulose matter were identified in the voids of the gel network, indicative of sufficient coverage of the whey protein surface.

The structuring synergism between WPI and FSM (Fig. 7) was associated with their behaviour towards segregative phase separation; for WPI to FSM ratios below 1:20 a significant increase (up to 7-fold) in the acid gels stiffness was observed. Exceeding the 1:20 WPI to FSM ratio, an abrupt reduction of the gels mechanical strength was observed with a subtle recovery of stiffness to occur at the highest FSM concentration tested. The adverse impact of segregative phase separation on the viscoelastic properties of protein gels has been well-demonstrated (Çakır & Foegeding, 2011; Pang, Deeth, & Bansal, 2015). When phase separation is primarily driven by depletion, the size of the biopolymer aggregates is the substantial parameter affecting the extent of phase separation contrarily to the subtle effect of temperature. In such case, gels prepared at 30 °C should be characterised by higher stiffness in accordance to the systems comprising less than 0.125% w/w FSM. Interestingly, on exceeding 0.125% of FSM a reversing effect of incubation temperature on the gels' viscoelastic properties i.e. stiffness was reduced on lowering incubation temperature, and thus, it is assumed that depletion induced phase separation is not the sole mechanism which impacted the viscoelastic properties of the gels. Trong Bach et al. (2014) showed that temperature dependent phase separation occurring in binary biopolymer systems, e.g. κ-carrageenan – β-lactoglobulin aggregates, is driven by the osmotic and elastic moduli. On temperature increase, biopolymers depletion may be sterically impeded beyond the gelation point and therefore, the adverse impact of phase separation on the microstructural and hence, on the mechanical properties of the acid gels. Further increase in the WPI to FSM ratio i.e. above 3:40 (which presumably refers to the narrow binodal curve region) was associated with the partial viscoelastic recovery of the gels, yet no evidence of structuring synergism between the whey proteins and flax seed mucilage was detected. The

CLSM micrographs of the FSM based acid gels revealed a good agreement between the colloidal aspects of the gels (Fig. 3) and the non-acidified binary biopolymer blends (Fig. 5). The latter suggests a fast progressing phase separation although the interplay between the gelation kinetics, and the microstructural and mechanical profile of the gels requires further investigation.

The WHC of the gels prepared at 30 °C and pre-conditioned at 25 °C for 3 h is illustrated in Suppl. Fig. 4. As shown, the WHC of the acid gels remained unchanged for both PSMs up to 0.05%. Despite the good water holding capacity of PSMs, on exceeding 0.05% w/w a gradual yet significant reduction of the gels WHC was observed. However, it should be noted that in the case of CSM the adverse effect on WHC was reversed above 0.375% whereas an improvement of the gels WHC was observed at the highest CSM concentration. Whey separation is associated with the extent of the rearrangement of the aggregated microparticles in the gel network formed (Lucey, 2001). It is well established that the compositional aspects of the gels together with the pre- and post-gelation processing conditions are the most influential parameters on WHC of cold-set protein gels. Although food polysaccharides may impart satisfactory textural, structural and organoleptic properties to dairy acid gels, on many occasions they may reduce the gels stability against gravitational serum separation (Pang et al., 2015; Soukoulis et al., 2007). Lucey (2001) reported that the rearrangement of the protein networks after gelation indicated by an increase in the loss tangent (tanδ) of the gels is associated to their serum expulsion proneness. As illustrated in Fig. 8, a negative correlation between the WHC and the loss tangent of the CSM based acid gels, and hence, it can be assumed that the WHC was associated with the ability of the CSM to sterically impede the rearrangement of the whey protein aggregates in the formed gel network and to bind water similarly to other adsorbing polysaccharides (Everett & McLeod, 2005; Pang et al., 2015). The latter mechanism appears to be partially confirmatory as concerns the impact of FSM on the

gels WHC: exceeding 0.375% the linearity between WHC and tanδ correlation was lost. Considering that phase separation was very evident above 0.375% of FSM, it is assumed that depletion of the non-adsorbed FSM leads to smaller whey protein aggregate crosslinks inducing loss of structural integrity (gels become more liquid-like) and eventually to serum expulsion.

4. CONCLUSIONS

The structuring and stabilising performance of PSMs in whey protein cold-set gels is essentially driven by the mucilage type and the WPI to PSM ratio. Although at very low concentrations (<0.05%) the presence of PSM was rather non-influential on soluble protein aggregates, at higher contents they were able to induce either associative (electrostatic bridging via positively charged patches on protein molecules and negative charge bearing PSM carboxyl groups) or segregative phase separation induced interactions. The associative interactions between PSM and whey proteins promoted early gelation. On the other hand, the gelation rates were declined on increasing PSM concentrations which was associated with the reduction of the crosslinking ability of whey proteins due to either the occurrence of depletion destabilisation (i.e. FSM) or the imposition of steric hindrances due to the substantial increase in the serum viscoelasticity (i.e. CSM). The presence of CSM enhanced acid gels stiffness was attributed to its adsorbing ability onto whey proteins below their isoelectric point promoting bridging of protein aggregates at lower CSM concentrations followed by their steric stabilisation at higher concentrations of CSM. Although FSM exerted also a good protein adsorbing capacity its structuring synergism was observed at concentrations below 0.25% suggesting that the occurrence of segregative phase separation results in a significant loss of structural integrity.

CONFLICTS OF INTEREST: The authors declare no conflicts of interest.

495 5. REFERENCES

496 Abaee, A., Mohammadian, M., & Jafari, S. M. (2017). Whey and soy protein-based hydrogels
497 and nano-hydrogels as bioactive delivery systems. *Trends in Food Science &*
498 *Technology*, *70*, 69–81.

499 Adibnia, V., & Hill, R. J. (2016). Universal aspects of hydrogel gelation kinetics, percolation
500 and viscoelasticity from PA-hydrogel rheology. *Journal of Rheology*, *60*(4), 541–548.

501 Albalasmeh, A. A., Berhe, A. A., & Ghezzehei, T. A. (2013). A new method for rapid
502 determination of carbohydrate and total carbon concentrations using UV
503 spectrophotometry. *Carbohydrate Polymers*, 97(2), 253–261.

504 Alting, A. C., Hamer, R. J., de Kruif, C. G., & Visschers, R. W. (2000). Formation of Disulfide
505 Bonds in Acid-Induced Gels of Preheated Whey Protein Isolate. *Journal of Agricultural*
506 *and Food Chemistry*, *48*(10), 5001–5007.

507 Basiri, S., Haidary, N., Shekarforoush, S. S., & Niakousari, M. (2018). Flaxseed mucilage: A
508 natural stabilizer in stirred yogurt. *Carbohydrate Polymers*, *187*, 59–65.

509 Behrouzian, F., Razavi, S. M. A., & Phillips, G. O. (2014). Cress seed (*Lepidium sativum*)
510 mucilage, an overview. *Bioactive Carbohydrates and Dietary Fibre*, *3*(1), 17–28.

511 Burgain, J., Corgneau, M., Scher, J., & Gaiani, C. (2015). Chapter 20 - Encapsulation of
512 Probiotics in Milk Protein Microcapsules. In L. M. C. Sagis (Ed.), *Microencapsulation*
513 *and Microspheres for Food Applications* (pp. 391–406). San Diego: Academic Press.

514 Bustamante, M., Oomah, B. D., Rubilar, M., & Shene, C. (2017). Effective *Lactobacillus*
515 *plantarum* and *Bifidobacterium infantis* encapsulation with chia seed (*Salvia hispanica*
516 L.) and flaxseed (*Linum usitatissimum* L.) mucilage and soluble protein by spray
517 drying. *Food Chemistry*, *216*, 97–105.

518 Çakır, E., & Foegeding, E. A. (2011). Combining protein micro-phase separation and protein–
519 polysaccharide segregative phase separation to produce gel structures. *Food*
520 *Hydrocolloids*, *25*(6), 1538–1546.
521 Calvet, D., Wong, J. Y., & Giasson, S. (2004). Rheological Monitoring of Polyacrylamide
522 Gelation: Importance of Cross-Link Density and Temperature. *Macromolecules*,
523 *37*(20), 7762–7771.
524 Campos, B. E., Dias Ruivo, T., da Silva Scapim, M. R., Madrona, G. S., & de C. Bergamasco,
525 R. (2016). Optimization of the mucilage extraction process from chia seeds and
526 application in ice cream as a stabilizer and emulsifier. *LWT - Food Science and*
527 *Technology*, *65*(Supplement C), 874–883.
528 Capitani, M. I., Matus-Basto, A., Ruiz-Ruiz, J. C., Santiago-García, J. L., Betancur-Ancona,
529 D. A., Nolasco, S. M., … Segura-Campos, M. R. (2016). Characterization of
530 Biodegradable Films Based on *Salvia hispanica* L. Protein and Mucilage. *Food and*
531 *Bioprocess Technology*, *9*(8), 1276–1286.
532 Cavallieri, A. L. F., & da Cunha, R. L. (2008). The effects of acidification rate, pH and ageing
533 time on the acidic cold set gelation of whey proteins. *Food Hydrocolloids*, *22*(3), 439–
534 448.
535 Corredig, M., Sharafbafi, N., & Kristo, E. (2011). Polysaccharide–protein interactions in dairy
536 matrices, control and design of structures. *Food Hydrocolloids*, *25*(8), 1833–1841.
537 Cui, S. W., Eskin, M. A. N., Wu, Y., & Ding, S. (2006). Synergisms between yellow mustard
538 mucilage and galactomannans and applications in food products — A mini review.
539 *Advances in Colloid and Interface Science*, *128–130*(Supplement C), 249–256.
540 de Jong, S., Klok, H. J., & van de Velde, F. (2009). The mechanism behind microstructure
541 formation in mixed whey protein–polysaccharide cold-set gels. *Food Hydrocolloids*,
542 *23*(3), 755–764.

543 Eissa, A. S., & Khan, S. A. (2005). Acid-Induced Gelation of Enzymatically Modified,
544 Preheated Whey Proteins. *Journal of Agricultural and Food Chemistry*, *53*(12), 5010–
545 5017.
546 Everett, D. W., & McLeod, R. E. (2005). Interactions of polysaccharide stabilisers with casein
547 aggregates in stirred skim-milk yoghurt. *International Dairy Journal*, *15*(11), 1175–
548 1183.
549 Fernandes, S. S., & Salas-Mellado, M. de las M. (2017). Addition of chia seed mucilage for
550 reduction of fat content in bread and cakes. *Food Chemistry*, *227*, 237–244.
551 Girard, M., & Schaffer-Lequart, C. (2008). Attractive interactions between selected anionic
552 exopolysaccharides and milk proteins. *Food Hydrocolloids*, *22*(8), 1425–1434.
553 Girard, M., Turgeon, S. L., & Gauthier, S. F. (2002). Interbiopolymer complexing between β-
554 lactoglobulin and low- and high-methylated pectin measured by potentiometric titration
555 and ultrafiltration. *Food Hydrocolloids*, *16*(6), 585–591.
556 Goh, Kelvin K. T., Sarkar, A., & Singh, H. (2008). Chapter 12 - Milk protein–polysaccharide
557 interactions. In *Milk Proteins* (pp. 347–376). San Diego: Academic Press.
558 Goh, Kelvin Kim Tha, Matia-Merino, L., Chiang, J. H., Quek, R., Soh, S. J. B., & Lentle, R.
559 G. (2016). The physico-chemical properties of chia seed polysaccharide and its
560 microgel dispersion rheology. *Carbohydrate Polymers*, *149*(Supplement C), 297–307.
561 Kavanagh, G. M., Clark, A. H., & Ross-Murphy, S. B. (2000). Heat-Induced Gelation of
562 Globular Proteins: 4. Gelation Kinetics of Low pH β-Lactoglobulin Gels. *Langmuir*,
563 *16*(24), 9584–9594.
564 Kay, B. A., Trigatti, K., MacNeil, M. B., Klingel, S. L., Repin, N., Goff, H.D., Duncan, A. M.
565 (2017). Pudding products enriched with yellow mustard mucilage, fenugreek gum or
566 flaxseed mucilage and matched for simulated intestinal viscosity significantly reduce

567 postprandial peak glucose and insulin in adults at risk for type 2 diabetes. *Journal of*
568 *Functional Foods*, 37(Supplement C), 603–611.
569 Khalloufi, S., Corredig, M., Goff, H. D., & Alexander, M. (2009). Flaxseed gums and their
570 adsorption on whey protein-stabilized oil-in-water emulsions. *Food Hydrocolloids*,
571 *23*(3), 611–618.
572 Kharlamova, A., Chassenieux, C., & Nicolai, T. (2018). Acid-induced gelation of whey protein
573 aggregates: Kinetics, gel structure and rheological properties. *Food Hydrocolloids*, *81*,
574 263–272.
575 Kuhn, K. R., Cavallieri, Â. L. F., & da Cunha, R. L. (2011). Cold-set whey protein–flaxseed
576 gum gels induced by mono or divalent salt addition. *Food Hydrocolloids*, *25*(5), 1302–
577 1310.
578 Liu, G., Jæger, T. C., Nielsen, S. B., Ray, C. A., & Ipsen, R. (2018). Physicochemical properties
579 of milk protein ingredients and their acid gelation behavior in different ionic
580 environments. *International Dairy Journal,* 85, 16-20
581 Liu, J., Shim, Y. Y., Shen, J., Wang, Y., & Reaney, M. J. T. (2017). Whey protein isolate and
582 flaxseed (*Linum usitatissimum* L.) gum electrostatic coacervates: Turbidity and
583 rheology. *Food Hydrocolloids*, *64*, 18–27.
584 Lopes da Silva, J. A., Rao, M. A., & Fu, J. T. (1998). Rheology of structure development and
585 loss during gelation and melting. In *Phase/State Transitions in Foods* (Rao M.A., Hartel
586 R.W., pp. 111–128). New York: Marcel Dekker Inc.
587 Lucey, J. A. (2002). Formation and Physical Properties of Milk Protein Gels. *Journal of Dairy*
588 *Science*, *85*(2), 281–294.
589 Lucey, J. A., & Singh, H. (1997). Formation and physical properties of acid milk gels: a review.
590 *Food Research International*, *30*(7), 529–542.

591 Lucey, John A. (2001). The relationship between rheological parameters and whey separation
592 in milk gels. *Food Hydrocolloids*, *15*(4), 603–608.
593 Luo, J., Li, Y., Mai, Y., Gao, L., Ou, S., Wang, Y., & Peng, X. (2018). Flaxseed gum reduces
594 body weight by regulating gut microbiota. Journal of Functional Foods, 47, 136–142.
595 Martin, F., Cayot, N., Marin, A., Journaux, L., Cayot, P., Gervais, P., & Cachon, R. (2009).
596 Effect of oxidoreduction potential and of gas bubbling on rheological properties and
597 microstructure of acid skim milk gels acidified with glucono-δ-lactone. *Journal of*
598 *Dairy Science*, *92*(12), 5898–5906.
599 Meletharayil, G. H., Patel, H. A., & Huppertz, T. (2015). Rheological properties and
600 microstructure of high protein acid gels prepared from reconstituted milk protein
601 concentrate powders of different protein contents. *International Dairy Journal*, *47*, 64–
602 71.
603 Menga, V., Amato, M., Phillips, T. D., Angelino, D., Morreale, F., & Fares, C. (2017). Gluten-
604 free pasta incorporating chia (*Salvia hispanica* L.) as thickening agent: An approach to
605 naturally improve the nutritional profile and the in vitro carbohydrate digestibility.
606 *Food Chemistry*, *221*, 1954–1961.
607 Morell, P., & Fiszman, S. (2017). Revisiting the role of protein-induced satiation and satiety.
608 *Food Hydrocolloids*, *68*, 199–210.
609 Naji-Tabasi, S., & Razavi, S. M. A. (2017). Functional properties and applications of basil seed
610 gum: An overview. *Food Hydrocolloids*, *73*(Supplement C), 313–325.
611 Nicolai, T., Britten, M., & Schmitt, C. (2011). β-Lactoglobulin and WPI aggregates:
612 Formation, structure and applications. *Food Hydrocolloids*, *25*(8), 1945–1962.
613 Ould Eleya, M. M., Ko, S., & Gunasekaran, S. (2004). Scaling and fractal analysis of
614 viscoelastic properties of heat-induced protein gels. *Food Hydrocolloids*, *18*(2), 315–
615 323.

616 Pang, Z., Deeth, H., & Bansal, N. (2015). Effect of polysaccharides with different ionic charge
617 on the rheological, microstructural and textural properties of acid milk gels. *Food*
618 *Research International*, *72*, 62–73.
619 Pang, Z., Deeth, H., Sharma, R., & Bansal, N. (2015). Effect of addition of gelatin on the
620 rheological and microstructural properties of acid milk protein gels. *Food*
621 *Hydrocolloids*, *43*, 340–351.
622 Salgado-Cruz, M. de la P., Ramírez-Miranda, M., Díaz-Ramírez, M., Alamilla-Beltran, L., &
623 Calderón-Domínguez, G. (2017). Microstructural characterisation and glycemic index
624 evaluation of pita bread enriched with chia mucilage. *Food Hydrocolloids*, *69*, 141–
625 149.
626 Soukoulis, C., Panagiotidis, P., Koureli, R., & Tzia, C. (2007). Industrial Yogurt Manufacture:
627 Monitoring of Fermentation Process and Improvement of Final Product Quality.
628 *Journal of Dairy Science*, *90*(6), 2641–2654.
629 Soukoulis, C., Gaiani, C., & Hoffmann, L. (2018). Plant seed mucilage as emerging biopolymer
630 in food industry applications. *Current Opinion in Food Science*, *22*, 28–42.
631 Syrbe, A., Bauer, W. J., & Klostermeyer, H. (1998). Polymer Science Concepts in Dairy
632 Systems—an Overview of Milk Protein and Food Hydrocolloid Interaction.
633 *International Dairy Journal*, *8*(3), 179–193.
634 Tamargo, A., Cueva, C., Laguna, L., Moreno-Arribas, M. V., & Muñoz, L. A. (2018).
635 Understanding the impact of chia seed mucilage on human gut microbiota by using the
636 dynamic gastrointestinal model simgi®. *Journal of Functional Foods*, 50, 104–111.
637 Timilsena, Y. P., Wang, B., Adhikari, R., & Adhikari, B. (2016). Preparation and
638 characterization of chia seed protein isolate–chia seed gum complex coacervates. *Food*
639 *Hydrocolloids*, *52*(Supplement C), 554–563.

640 Trong Bach, N., Phan-Xuan, T., Benyahia, L., & Nicolai, T. (2014). Combined effects of
641 temperature and elasticity on phase separation in mixtures of κ-carragheenan and β-
642 lactoglobulin aggregates. *Food Hydrocolloids*, *34*, 138–144.
643 Western, T. L. (2012). The sticky tale of seed coat mucilages: production, genetics, and role in
644 seed germination and dispersal. *Seed Science Research*, *22*(1), 1–25.
645 Wijaya, W., Van der Meeren, P., & Patel, A. R. (2017). Cold-set gelation of whey protein
646 isolate and low-methoxyl pectin at low pH. *Food Hydrocolloids*, *65*, 35–45.
647 Ye, A. (2008). Complexation between milk proteins and polysaccharides via electrostatic
648 interaction: principles and applications – a review. *International Journal of Food*
649 *Science & Technology*, *43*(3), 406–415.

TABLE 1: Acidification kinetic parameters (calculated according to Eq. 1 and 2) of whey protein isolate aqueous systems as influenced by the presence of chia (CSM) or flaxseed (FSM) mucilage used in the range of 0.05 to 0.75% w/w.

Acid gel system		k_1 (h^{-1})	k_2 (h^{-1})	τ_c (h)	Total acidification time, t_{acid} (h^{-1})
Incubation temperature 30 °C					
	WPI	$3.92 \pm 0.09^{a,A}$	$0.087 \pm 0.003^{c,B}$	0.173	$2.13 \pm 0.11^{a,A}$
CSM	0.05%	3.91 ± 0.11^{a}	0.087 ± 0.002^{c}	0.174	2.29 ± 0.12^{ab}
	0.125%	4.06 ± 0.06^{a}	0.088 ± 0.002^{c}	0.167	2.46 ± 0.08^{bc}
	0.25%	3.74 ± 0.08^{a}	0.082 ± 0.003^{bc}	0.181	2.85 ± 0.06^{cd}
	0.375%	3.88 ± 0.09^{a}	0.078 ± 0.002^{abc}	0.175	2.98 ± 0.09^{de}
	0.5%	4.10 ± 0.13^{a}	0.072 ± 0.001^{ab}	0.166	3.03 ± 0.12^{de}
	0.75%	4.09 ± 0.07^{a}	0.065 ± 0.003^{a}	0.166	3.11 ± 0.08^{e}
	CSM mean	$3.96^{A\dagger}$	$0.078^{A\dagger}$	0.172	$2.78^{C\dagger}$
FSM	0.05%	3.86 ± 0.13^{a}	0.089 ± 0.002^{c}	0.175	2.14 ± 0.09^{a}
	0.125%	4.08 ± 0.09^{a}	0.089 ± 0.002^{c}	0.171	2.11 ± 0.11^{a}
	0.25%	3.86 ± 0.10^{a}	0.085 ± 0.001^{b}	0.176	2.55 ± 0.08^{bc}
	0.375%	4.81 ± 0.28^{b}	0.067 ± 0.006^{a}	0.142	3.11 ± 0.17^{e}
	0.5%	4.02 ± 0.10^{a}	0.091 ± 0.003^{c}	0.169	2.77 ± 0.06^{c}
	0.75%	4.34 ± 0.08^{a}	0.090 ± 0.001^{c}	0.171	2.44 ± 0.05^{bc}
	FSM mean	$4.17^{B\dagger}$	$0.085^{B\dagger}$	0.167	$2.52^{B\dagger}$
Incubation temperature 37 °C					
	WPI	3.84 ± 0.08^{a}	$0.111 \pm 0.002^{f,C}$	0.176	$1.77 \pm 0.07^{a,A}$
CSM	0.05%	3.96 ± 0.05^{ab}	0.111 ± 0.001^{f}	0.170	1.92 ± 0.08^{a}
	0.125%	3.92 ± 0.04^{a}	0.087 ± 0.002^{cd}	0.173	2.04 ± 0.09^{ab}
	0.25%	4.14 ± 0.09^{bc}	0.096 ± 0.001^{e}	0.164	2.12 ± 0.05^{b}
	0.375%	4.25 ± 0.06^{bc}	0.080 ± 0.002^{bc}	0.160	2.41 ± 0.12^{cd}
	0.5%	4.22 ± 0.07^{bc}	0.079 ± 0.001^{bc}	0.161	2.52 ± 0.16^{cde}
	0.75%	4.09 ± 0.12^{c}	0.082 ± 0.001^{ab}	0.157	2.56 ± 0.04^{d}
	CSM mean	$4.10^{B\ddagger}$	$0.089^{A\ddagger}$	0.164	$2.26^{B\ddagger}$
FSM	0.05%	3.93 ± 0.05^{a}	0.102 ± 0.003^{f}	0.172	1.81 ± 0.09^{a}
	0.125%	3.96 ± 0.06^{ab}	0.099 ± 0.001^{e}	0.171	1.91 ± 0.11^{a}
	0.25%	3.97 ± 0.03^{ab}	0.089 ± 0.001^{d}	0.170	2.11 ± 0.06^{b}
	0.375%	4.81 ± 0.04^{d}	0.069 ± 0.001^{a}	0.142	2.91 ± 0.16^{ef}
	0.5%	4.71 ± 0.09^{d}	0.102 ± 0.002^{f}	0.143	2.74 ± 0.11^{e}
	0.75%	4.07 ± 0.07^{ab}	0.071 ± 0.001^{ef}	0.166	2.22 ± 0.06^{bc}
	FSM mean	$4.24^{C\ddagger}$	$0.097^{B\ddagger}$	0.161	$2.28^{B\ddagger}$

[a, A] Different letter between the rows indicate significant differences according to Tukey's post hoc means comparison test.

[†, ‡] Different symbol between CSM and FSM mean values indicates significant differences as concerns to incubation temperature

TABLE 2: Elastic modulus G′ frequency dependency parameters calculated using the Winter-Chambon model (Eq. 3) of the whey protein acid gels as influenced by the presence of chia (CSM) or flaxseed (FSM) mucilage (used in the range of 0.125 to 0.75% w/w). The protein gels were pre-conditioned at 25 °C for 2 h prior analyses.

Acid gel system		K' (Pa·Hz$^{-n^*}$)	n'	R^2
Incubation temperature 30°C				
WPI		337 ± 16^{c,A}	0.120 ± 0.001^{d,A}	0.997
CSM	0.125%	1137 ± 24^{d}	0.107 ± 0.002^{b}	0.994
	0.25%	2440 ±17^{h}	0.107 ± 0.002^{b}	0.999
	0.375%	1887 ± 62^{e}	0.114 ± 0.001^{bcd}	0.995
	0.5%	2298 ± 44^{g}	0.134 ± 0.003^{e}	0.959
	0.75%	1817 ± 32^{e}	0.078 ± 0.004^{a}	0.967
	CSM mean	*1456^{C}*	*0.108^{B}*	
FSM	0.125%	1137 ± 17^{d}	0.107 ± 0.002^{b}	0.997
	0.25%	2033 ± 36^{f}	0.110 ± 0.001^{bc}	0.999
	0.375%	119 ± 7^{b}	0.117 ± 0.003^{cd}	0.992
	0.5%	23.5 ± 1.2^{a}	0.145 ± 0.006^{f}	0.950
	0.75%	64.5 ± 3.2^{ab}	0.132 ± 0.004^{e}	0.992
	FSM mean	*675^{B†}*	*0.122^{A†}*	
Incubation temperature 37°C				
WPI		260 ± 11^{b,A}	0.112 ± 0.001^{d}	0.999
CSM	0.125%	953 ± 29^{c}	0.110 ± 0.002^{d}	0.992
	0.25%	2358 ± 32^{g}	0.095 ± 0.002^{c}	0.993
	0.375%	2216 ± 41^{f}	0.089 ± 0.002^{b}	0.990
	0.5%	2562 ± 8^{h}	0.081 ± 0.001^{a}	0.972
	0.75%	2561 ± 48^{h}	0.081 ± 0.003^{a}	0.972
	CSM mean	*2130^{C}*	*0.091^{A}*	
FSM	0.125%	1824 ± 32^{e}	0.111 ± 0.001^{d}	0.991
	0.25%	1071 ± 12^{d}	0.112 ± 0.001^{d}	0.989
	0.375%	76.4 ± 5.8^{a}	0.111 ± 0.002^{d}	0.973
	0.5%	12.3 ± 0.7^{a}	0.147 ± 0.002^{e}	0.889
	0.75%	188 ± 10^{b}	0.115 ± 0.001^{d}	0.995
	FSM mean	*634^{B†}*	*0.119^{B†}*	

$^{a, A}$ Different letter between the rows indicate significant differences according to Tukey's post hoc means comparison test.

$^{\dagger, \ddagger}$ Different symbol between CSM and FSM mean values indicates significant differences as concerns to incubation temperature

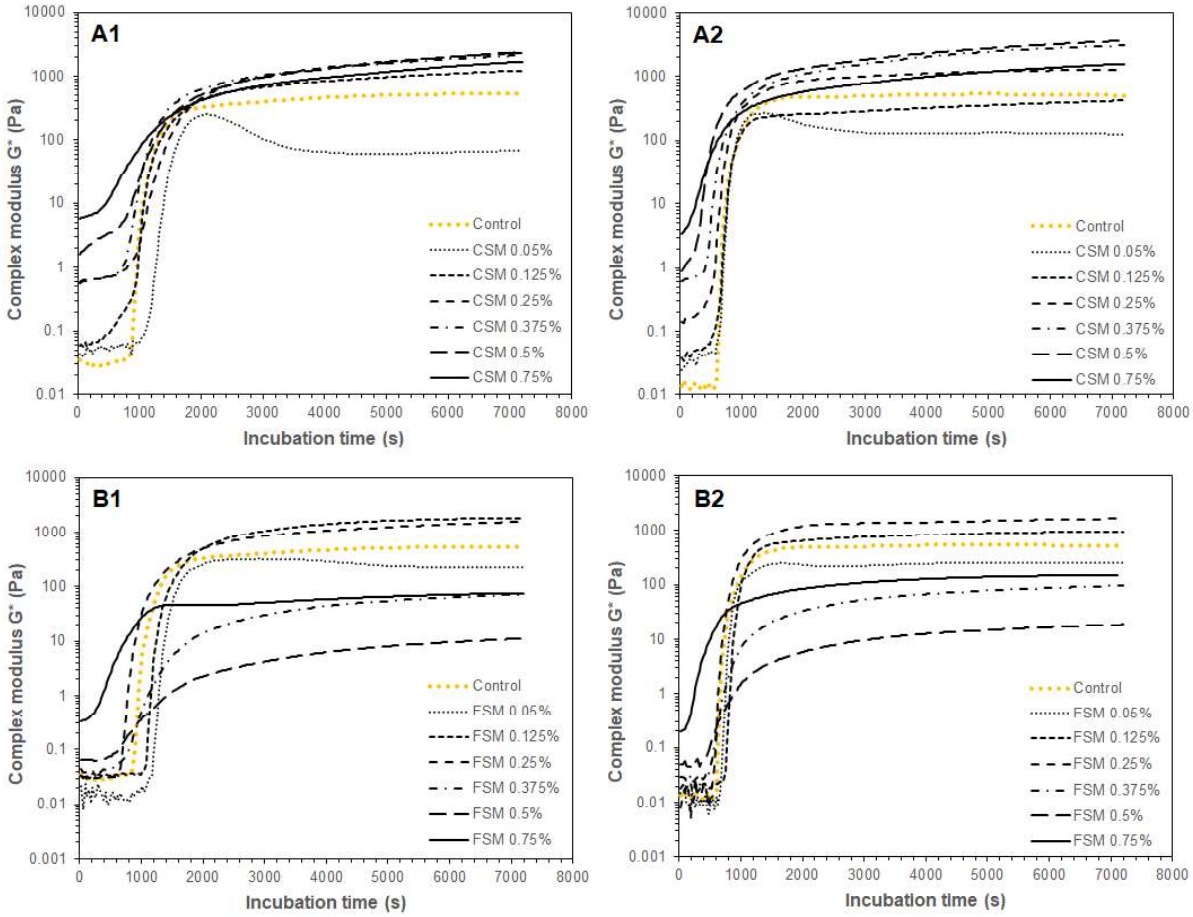

FIGURE 1: Complex modulus (G*) evolution throughout δ-glucono-lactone induced acidification (1 = 30 °C, 2 = 37 °C) of whey protein isolate as influenced by the presence of chia seed (A) or flaxseed (B) mucilage.

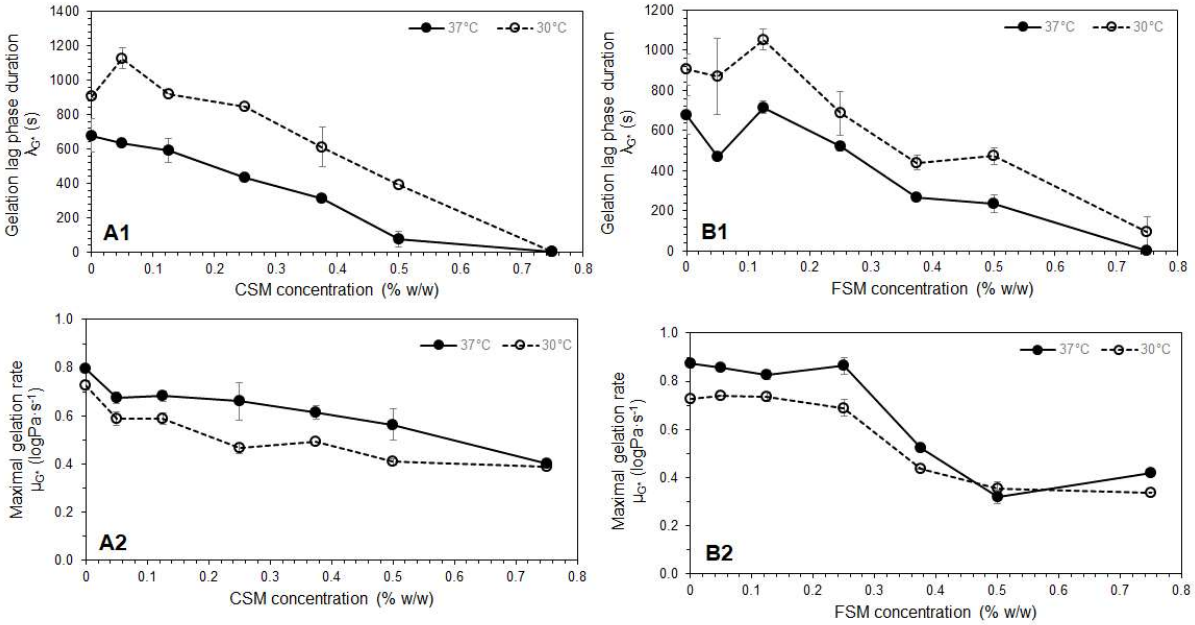

FIGURE 2: Gelation kinetic parameters (gelation lag phase duration λ_{G*} and maximal gelation rate, μ_{G*}) of whey protein isolate in the presence of chia seed (A) or flaxseed (B) mucilage as determined using the modified Gompertz model (Eq. 6). Acid gelation was conducted either at 30 °C (1) or 37 °C (2).

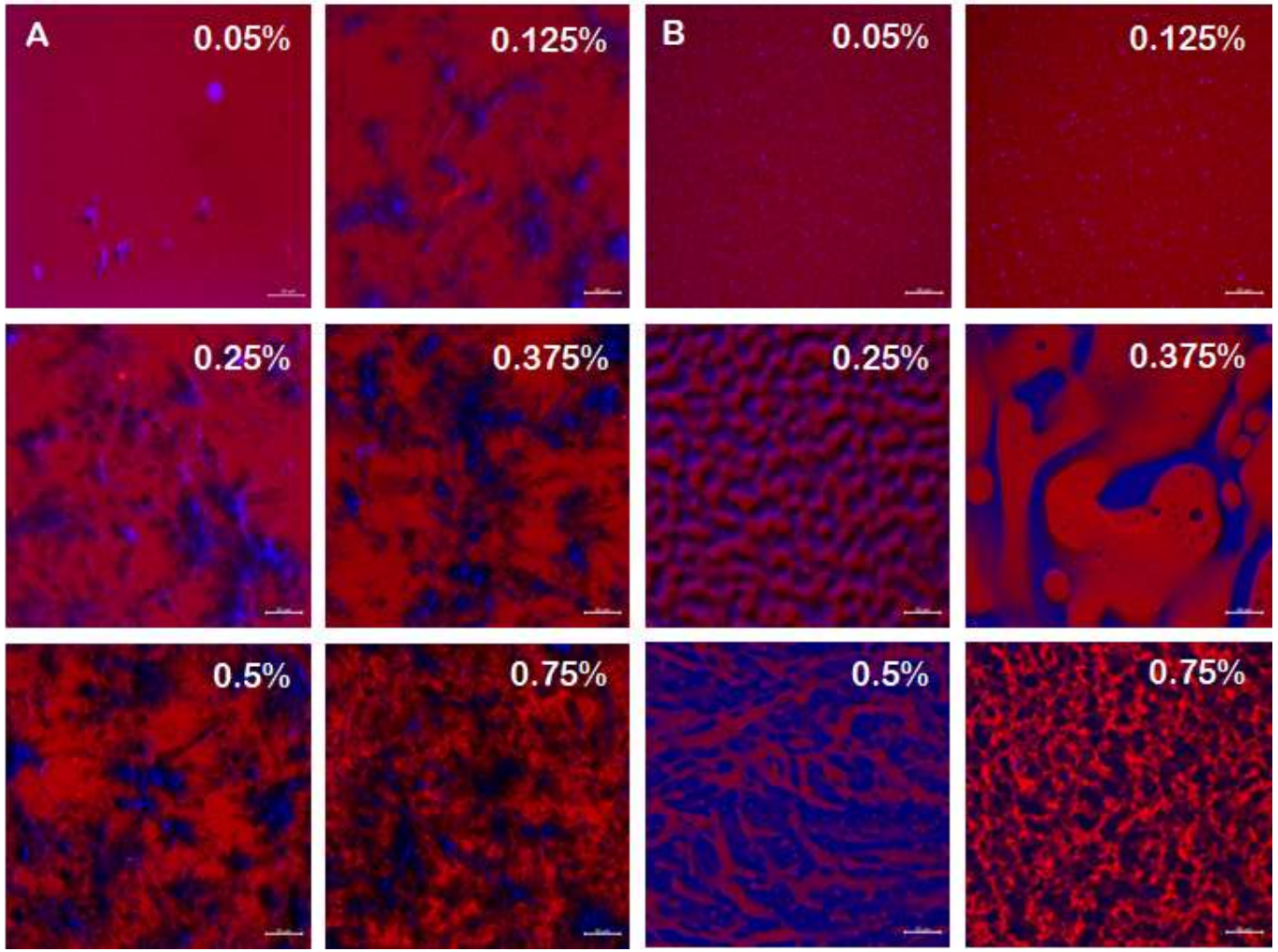

FIGURE 3: CLSM micrographs of whey protein – plant seed mucilage binary blends (A: chia seed, B: flaxseed) conditioned at 30 °C for 1 h. Whey proteins were stained with Fast Green (excited at 633 nm) whilst the hemicellulose mucilage fraction was stained with Calcofluor White (excited at 405 nm). Protein rich and mucilage rich micro-domains are illustrated in red and blue colour respectively. Scale bar = 50 μm

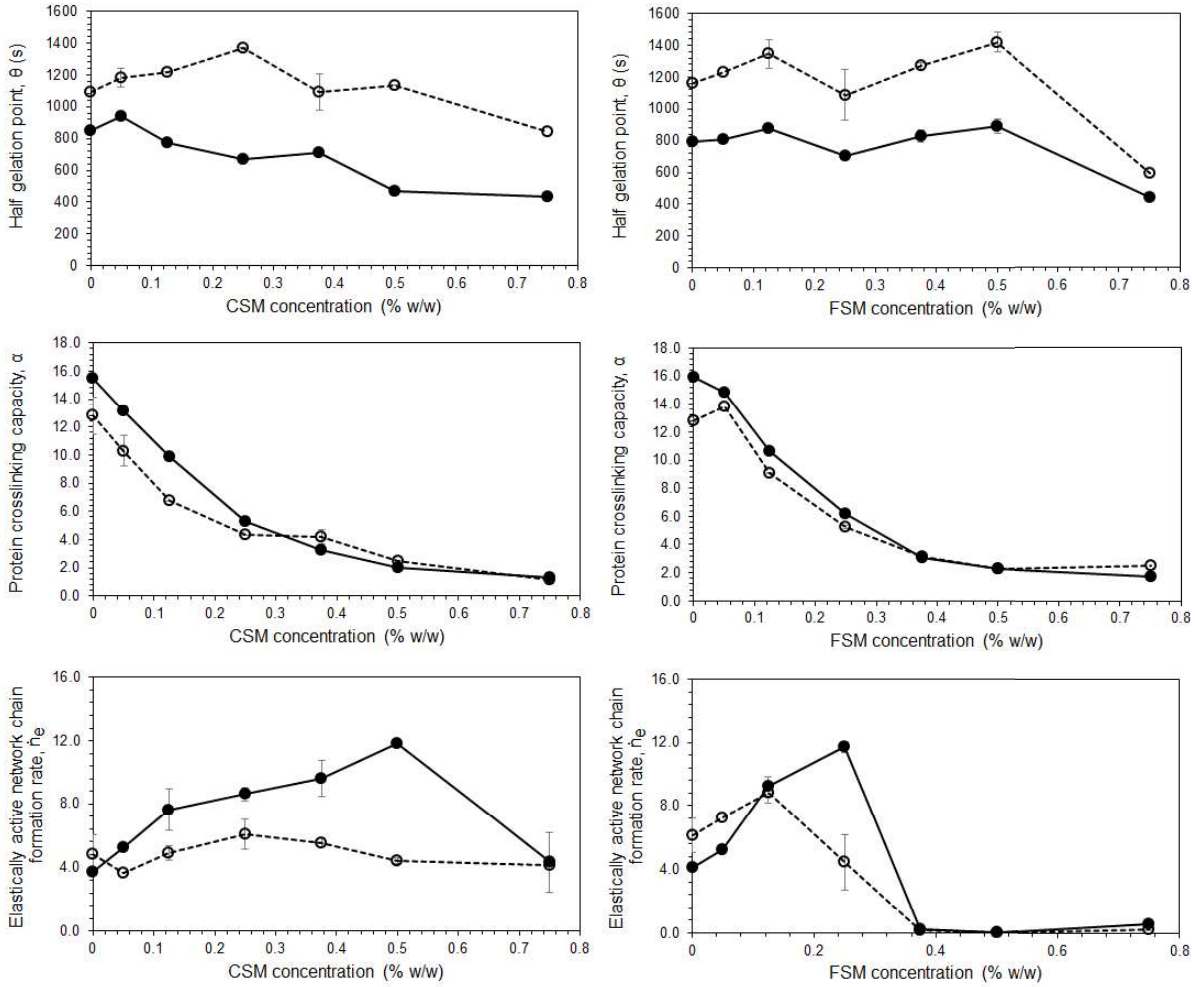

FIGURE 4: Gelation half-time (θ), protein crosslinking capacity (α) and formation rates of elastically active network chains ($\dot{n}_e$) values calculated according to the cascade theory model (Eq. 8) as influenced by incubation temperature (open symbols: 30 °C, closed symbols: 37 °C), plant seed mucilage type (chia vs. flaxseed) and concentration.

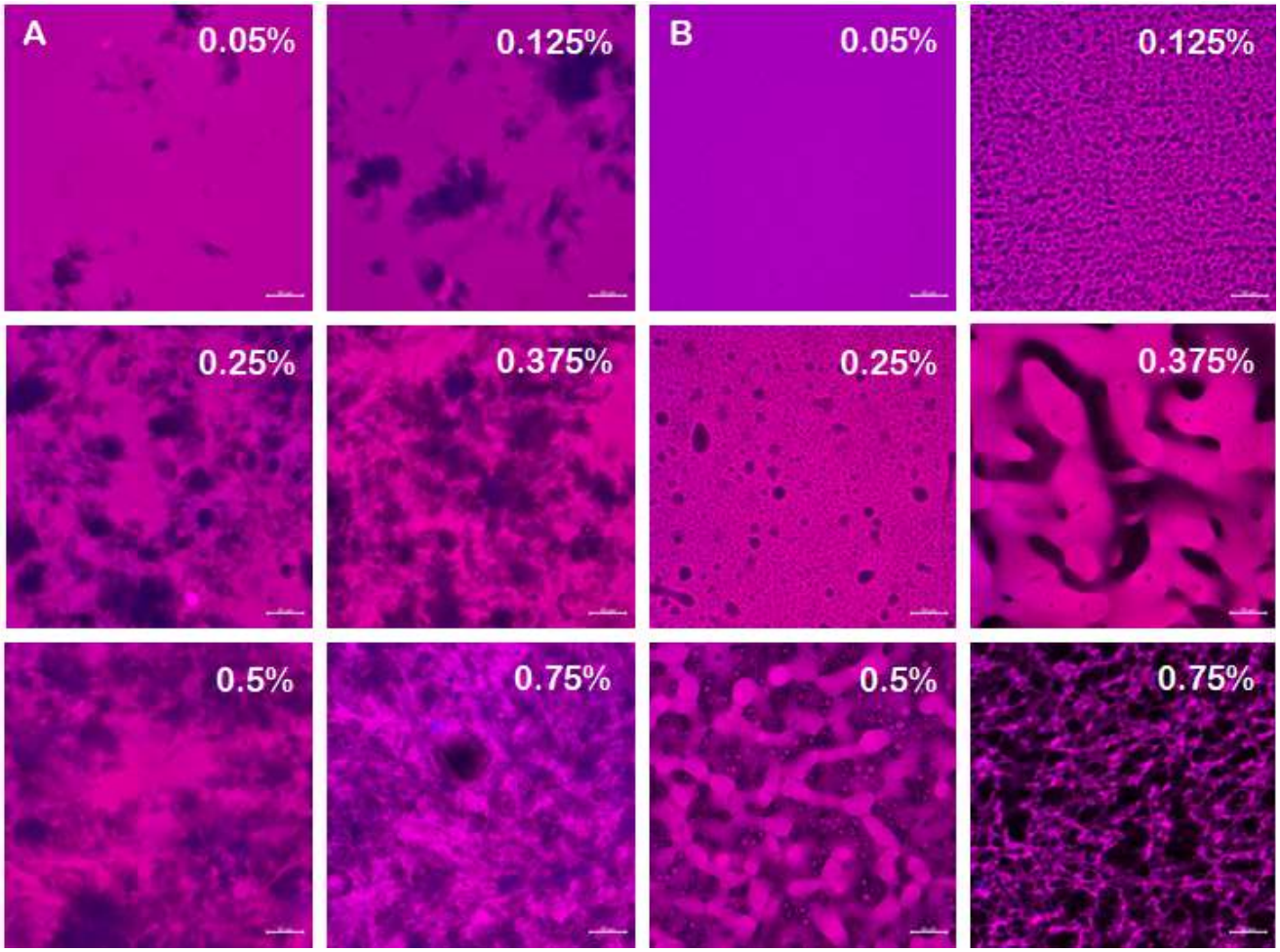

FIGURE 5: CLSM micrographs of whey protein – plant seed mucilage acid gels (A: chia seed, B: flaxseed) produced at 30 °C. Whey proteins were stained with Fast Green (excited at 633 nm) whilst the hemicellulose fraction of mucilage is stained with Calcofluor White (excited at 405 nm). Whey protein – mucilage adsorbed rich microdomains are visualised in purple whereas blue colour indicates non-adsorbed mucilage Scale bar = 50 μm

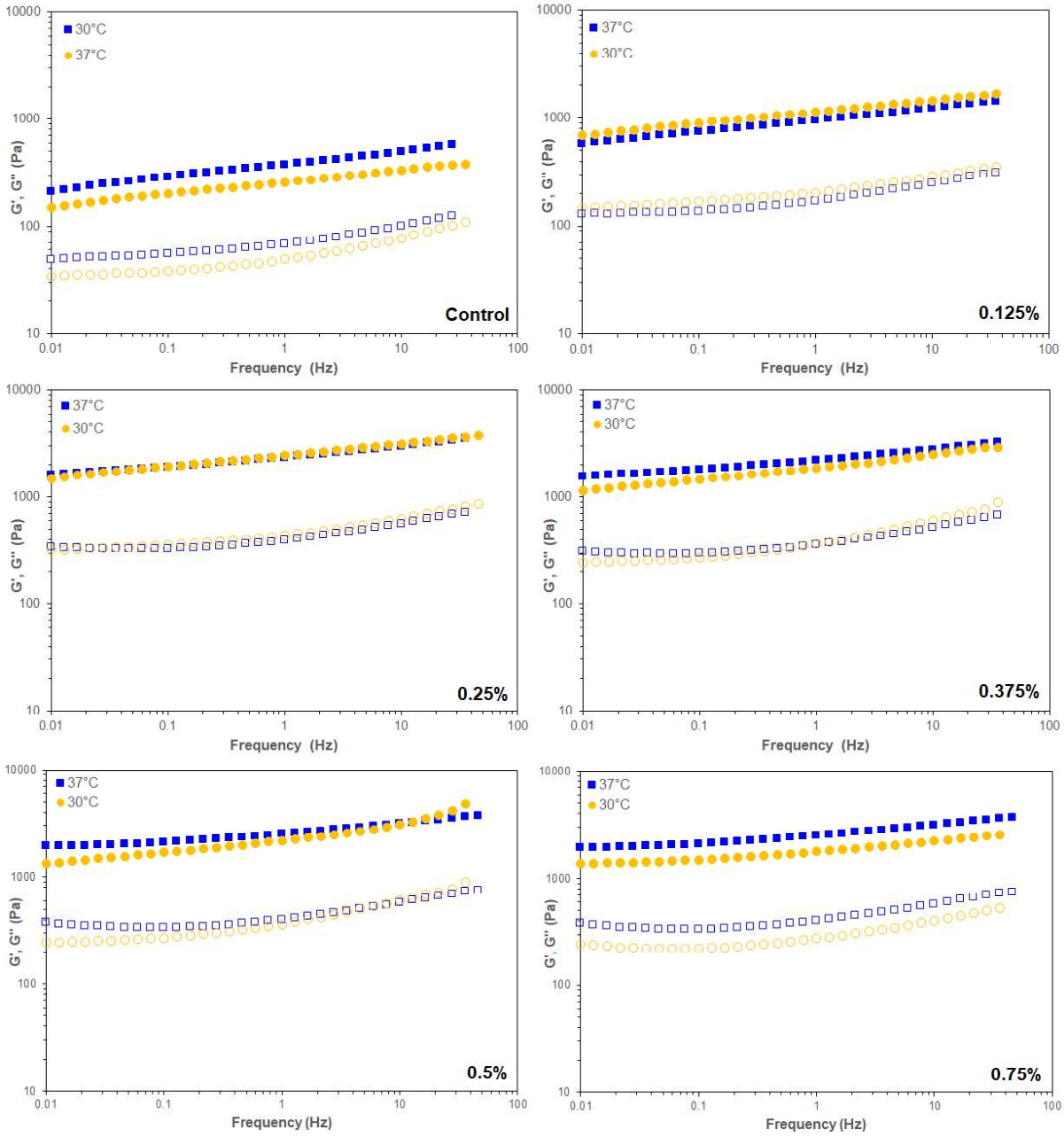

FIGURE 6: Frequency dependence of the elastic (G′, closed symbols) and viscous (G′′, open symbols) moduli (strain 0.5%) of chia seed mucilage co-structured (in the range of 0.125 to 0.75% w/w) whey protein acid gels pre-conditioned at 30 °C for 30 min following incubation (pH_{end} = 4.5) at 30 (circles) or 37 °C (squares) respectively.

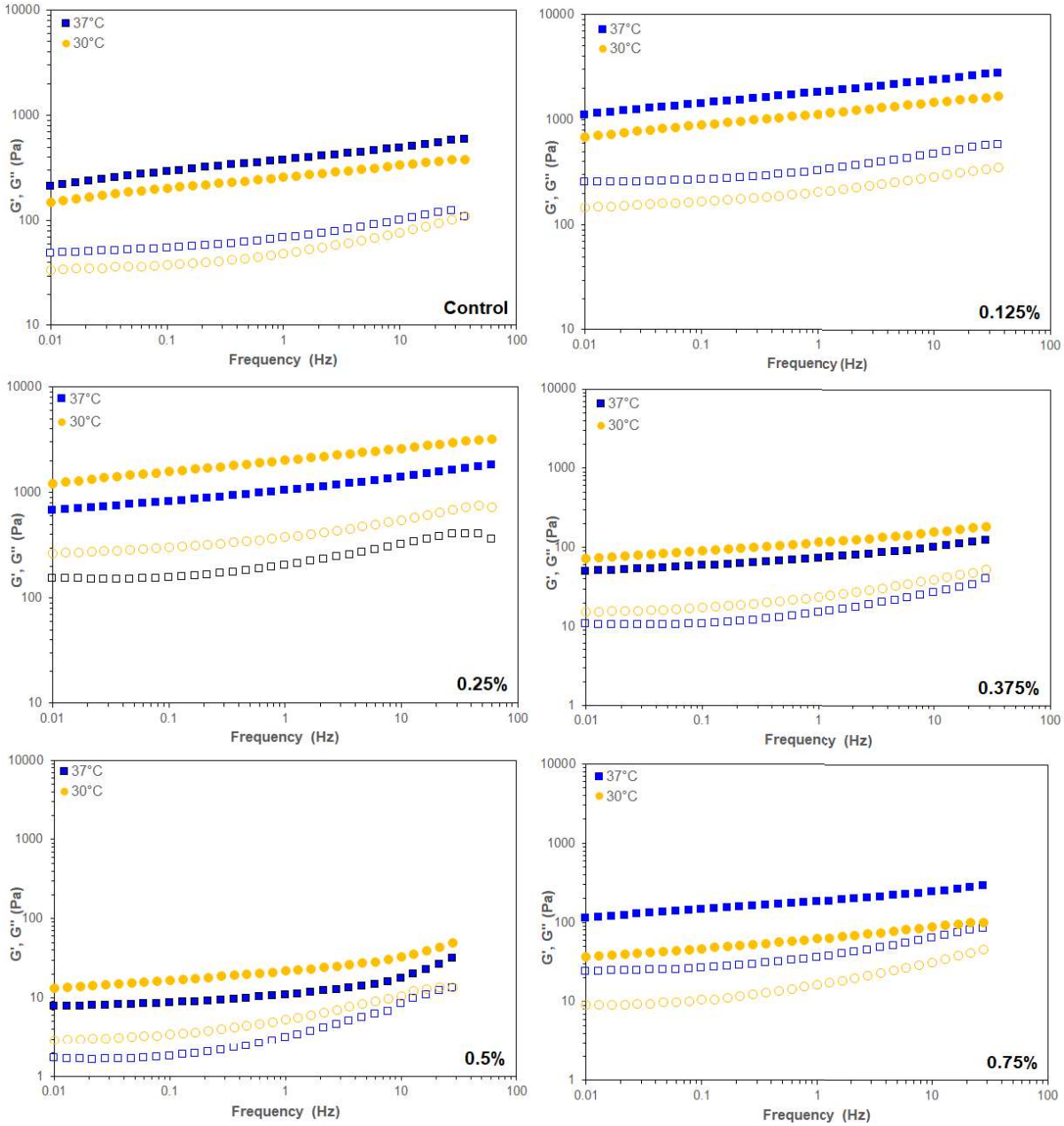

FIGURE 7: Frequency dependence of the elastic (G′, closed symbols) and viscous (G″, open symbols) moduli (strain 0.5%) of flaxseed mucilage co-structured (in the range of 0.125 to 0.75% w/w) whey protein acid gels pre-conditioned at 30 °C for 30 min following incubation (pH_{end} = 4.5) at 30 (circles) or 37 °C (squares) respectively.

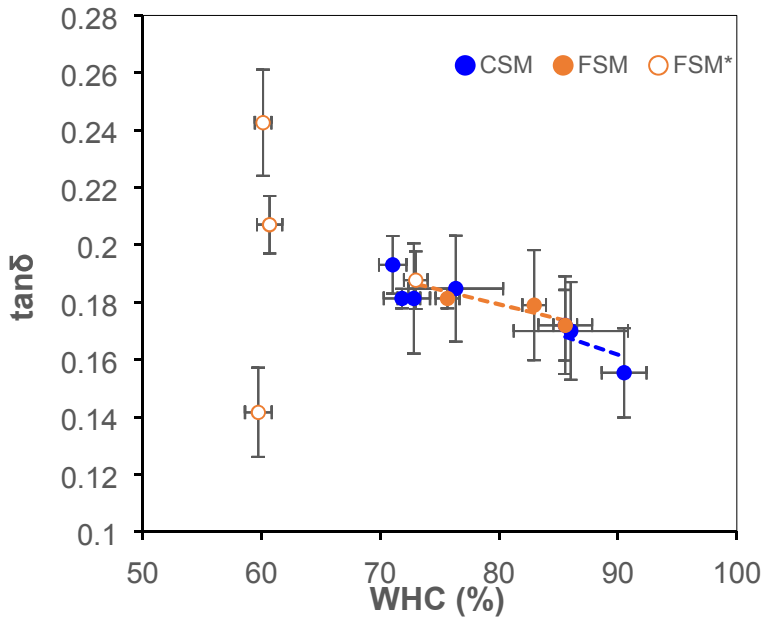

FIGURE 8: Interrelationship between the water holding capacity (WHC) and loss tangent (tanδ) of the acid gels (incubated at 30 °C and preconditioned at the 25 °C for 3 h) as influenced by the plant seed mucilage type and content. The open points illustrate acid gels in which phase separation was detected.

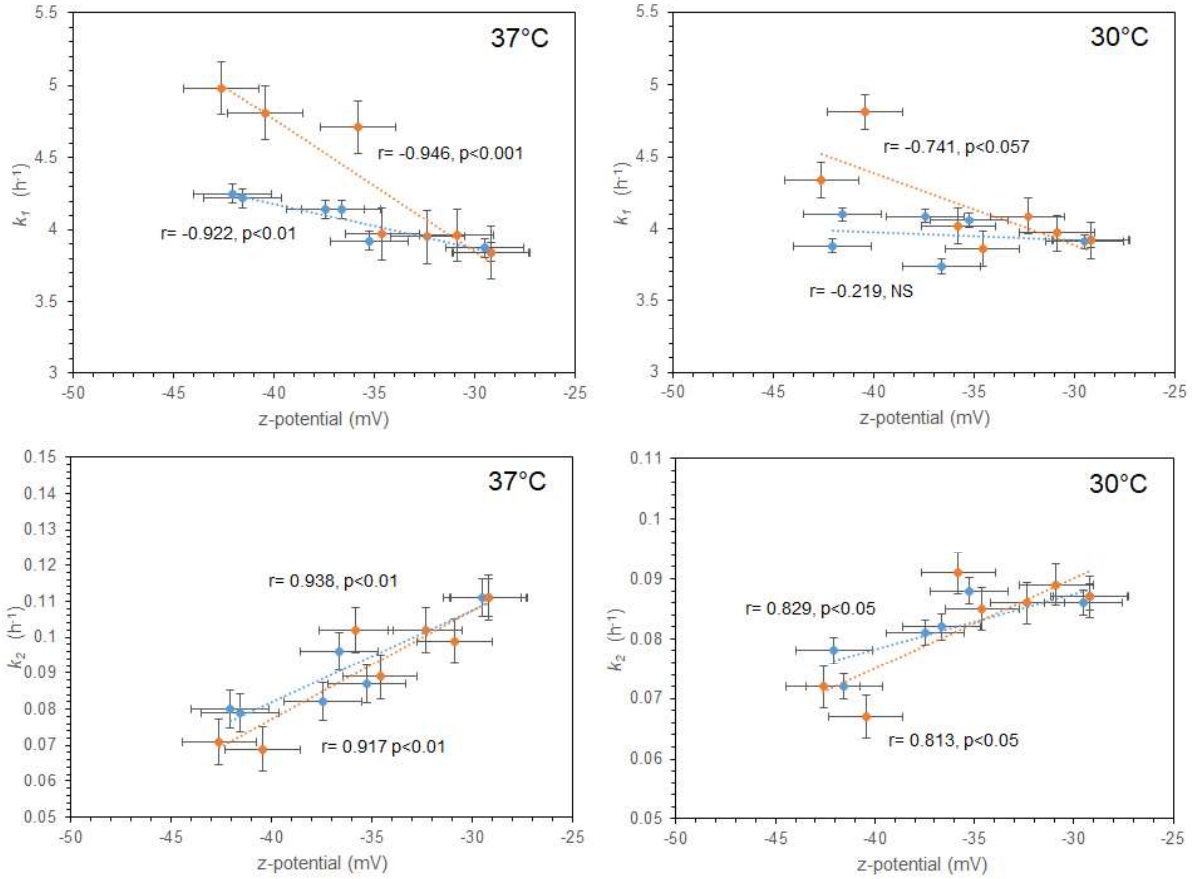

SUPPLEMENTARY FIGURE 1: Correlation of acidification rates (k_1 and k_2) to the ζ-potential values of the binary WPI/PSM systems (blue = chia seed mucilage, orange = flaxseed) using the Pearson's correlation test. Values refer to means ± standard error.

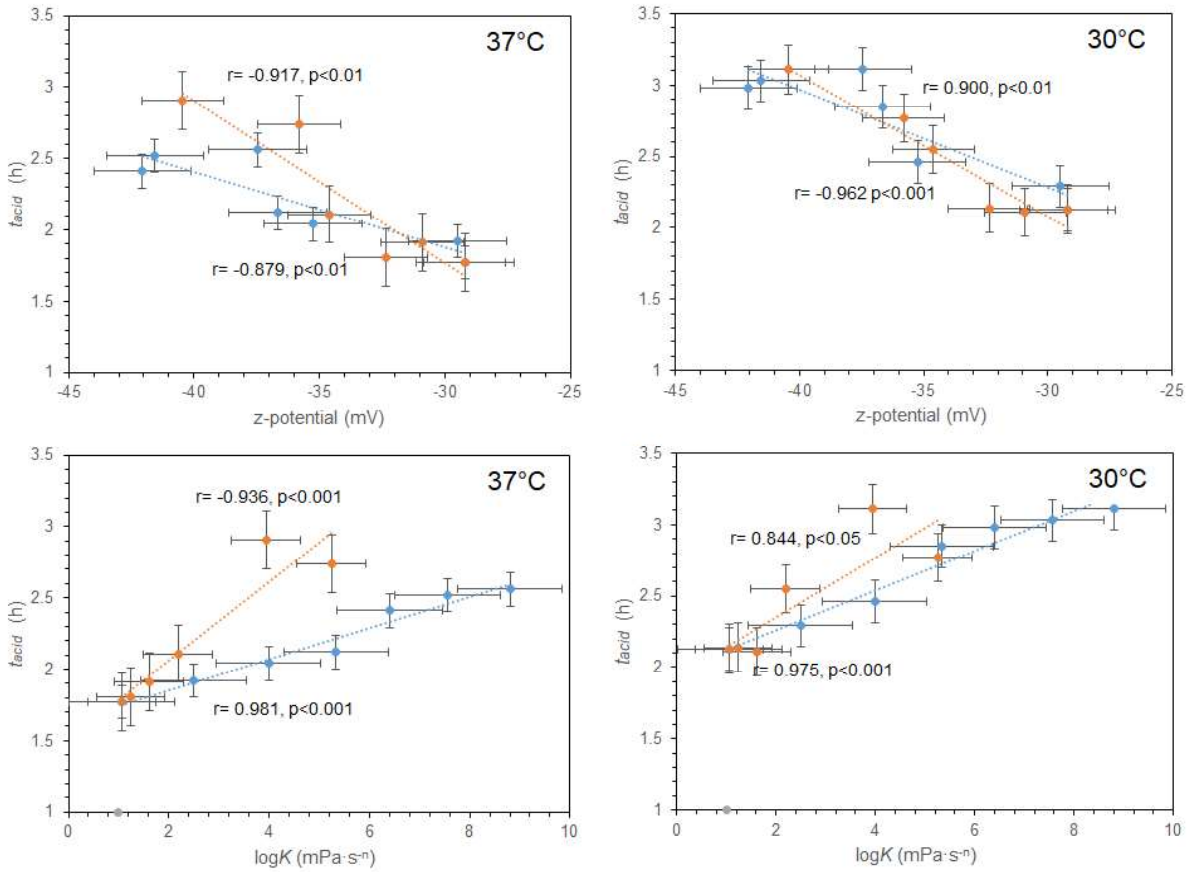

SUPPLEMENTARY FIGURE 2: Correlation of acidification time (t_{acid}) to the ζ-potential and flow consistency coefficient (log*K*) values of the binary WPI/PSM systems (blue = chia seed mucilage, orange = flaxseed) using the Pearson's correlation test. Values refer to means ± standard error.

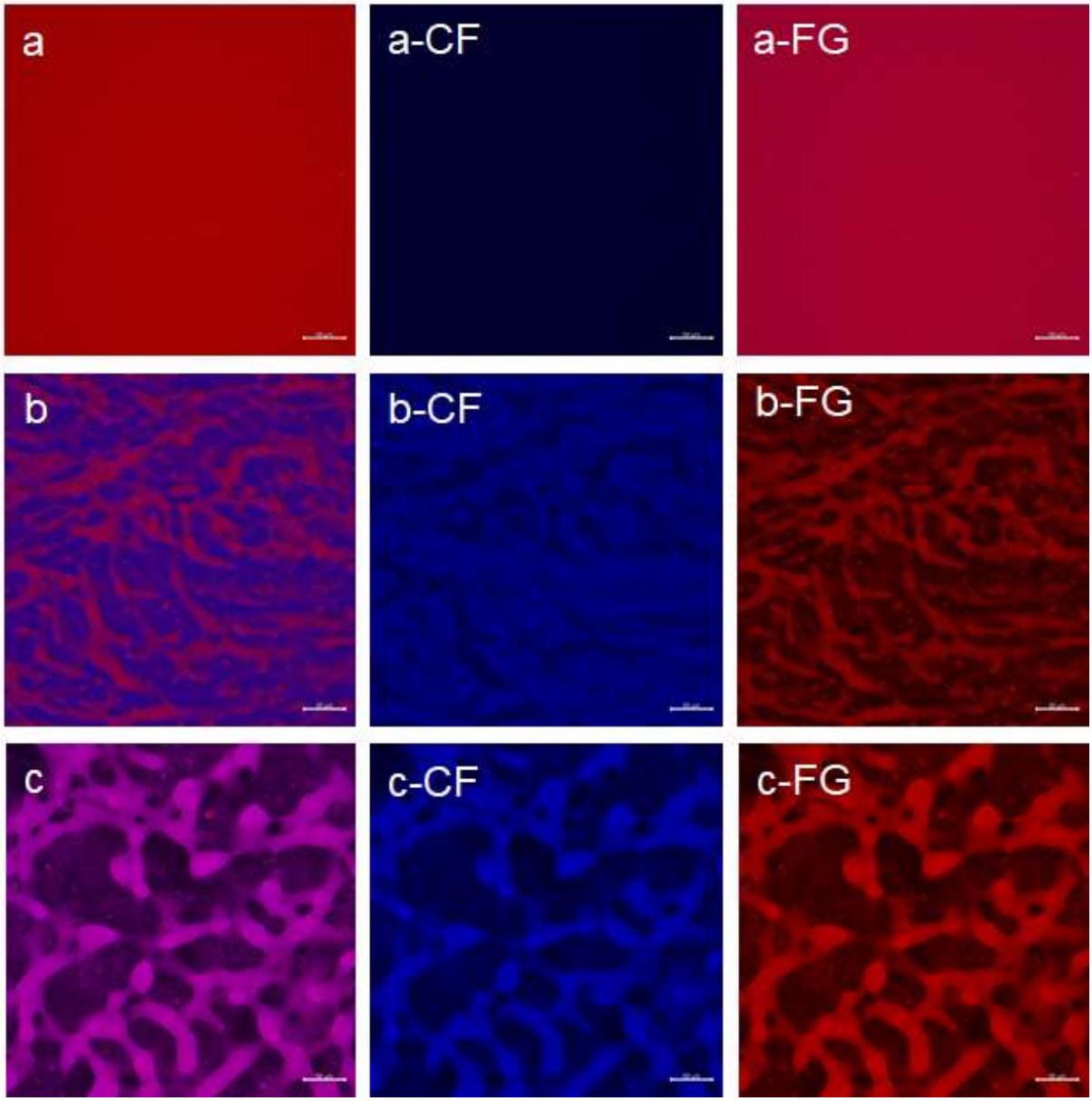

SUPPLEMENTARY FIGURE 3: a: WPI acid gel, b: 0.5% FSM – WPI aqueous system (30 °C for 1 h), and c: 0.5% FSM – WPI acid gel. CF: micro-domains where Calcofluor White is bound, FG: micro-domains where Fast Green FCF is bound.

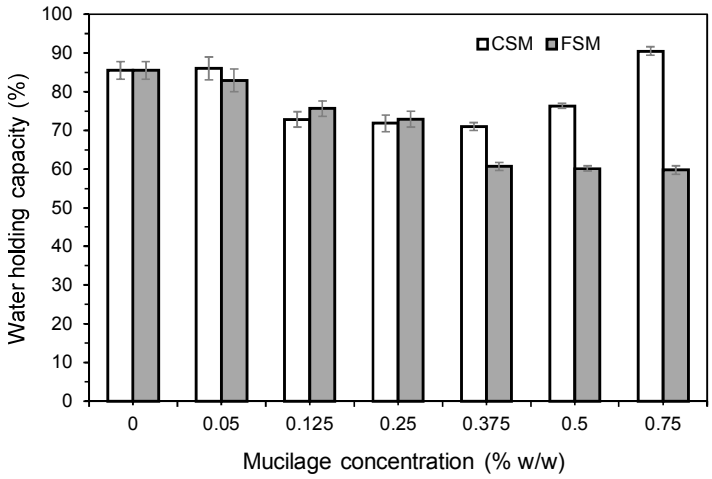

SUPPLEMENTARY FIGURE 4: Water holding capacity of acid whey-protein gels (produced at 30°C and pre-conditioned at 25 °C for 3 h) co-structured with either chia seed (CSM) or flax seed (FSM) mucilage.